Patchy deletion of Bmpr1a potentiates proximal pulmonary artery remodeling in mice exposed to chronic hypoxia
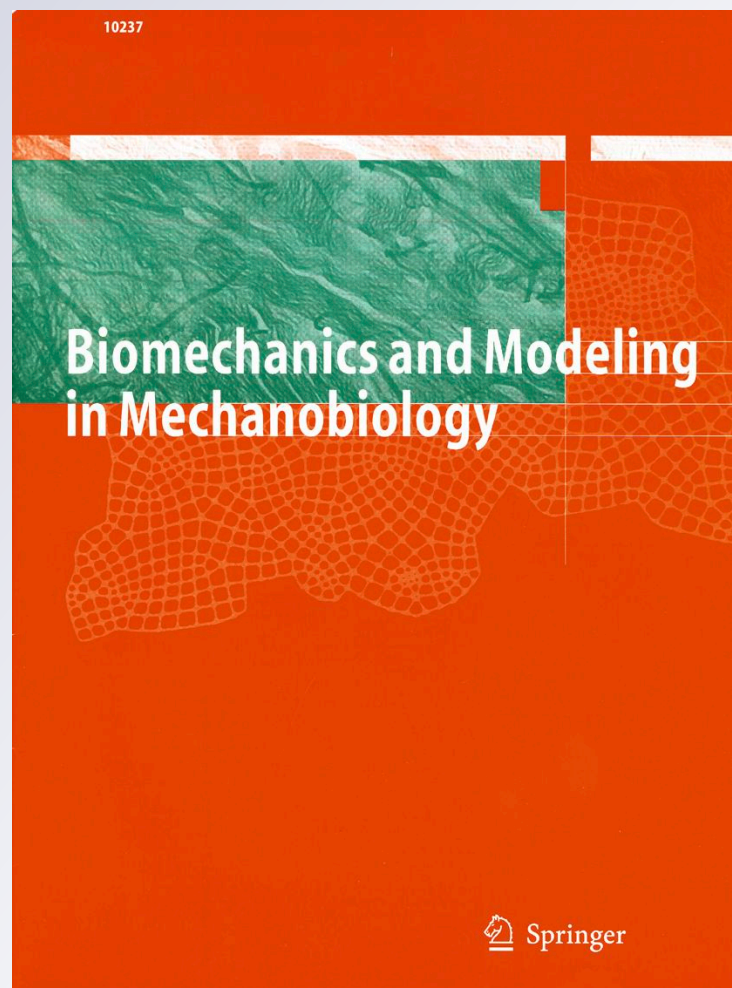
Rebecca R. Vanderpool, Nesrine El-Bizri, Marlene Rabinovitch & Naomi C. Chesler

10237

Biomechanics and Modeling in Mechanobiology

Springer

Springer

Springer

ORIGINAL PAPER

Patchy deletion of Bmpr1a potentiates proximal pulmonary artery remodeling in mice exposed to chronic hypoxia

**Rebecca R. Vanderpool · Nesrine El-Bizri ·
Marlene Rabinovitch · Naomi C. Chesler**

Abstract Reduced vascular expression of bone morphogenetic protein type IA receptor (*Bmpr1a*) has been found in patients with pulmonary arterial hypertension. Our previous studies in mice with patchy deletion of *Bmpr1a* in vascular smooth muscle cells and cardiac myocytes showed decreased distal vascular remodeling despite a similar severity of hypoxic pulmonary hypertension (HPH). We speculate increased stiffness from ectopic deposition of collagen in proximal pulmonary arteries might account for HPH. Pulsatile pressure-flow relationships were measured in isolated, ventilated, perfused lungs of $SM22\alpha;TRE\text{-}Cre;R26R;Bmpr1a^{flox/flox}$ (KO) mice and wild-type littermates, following 21 days (hypoxia) and 0 days (control) of chronic hypoxia. Pulmonary vascular impedance, which yields insight into proximal and distal arterial remodeling, was calculated. Reduced *Bmpr1a* expression had no effect on input impedance Z_0 ($P = 0.52$) or characteristic impedance Z_C ($P = 0.18$) under control conditions; it also had no effect on the decrease in Z_0 via acute rho kinase inhibition. However, following chronic hypoxia, reduced *Bmpr1a* expression increased Z_C ($P < 0.001$) without affecting Z_0 ($P = 0.72$). These results demonstrate that *Bmpr1a* deficiency does not significantly alter the hemodynamic function of the distal vasculature or its response to chronic hypoxia but larger, more proximal arteries are affected. In particular, reduced *Bmpr1a* expression likely decreased dilatation and increased stiffening in

response to hypoxia, probably by collagen accumulation. Increased PA stiffness can have a significant impact on right ventricular function. This study illustrates for the first time how proximal pulmonary artery changes in the absence of distal pulmonary artery changes contribute to pulmonary arterial hypertension.

1 Introduction

Pulmonary arterial hypertension (PAH) is a relatively rare but fatal disease in which mean pulmonary arterial pressure exceeds 25 mmHg and pulmonary capillary wedge pressure is less than 15 mmHg (McLaughlin et al. 2009). PAH is associated with significant pulmonary vascular remodeling, which increases right ventricular afterload and impairs right ventricular function, eventually leading to right ventricular failure. The prognosis for PAH is quite poor; even with modern treatment options, the one-year mortality rate is about 15% (McLaughlin et al. 2009). Currently, the best predictor of mortality from PAH is large, extralobar artery stiffness (Gan et al. 2007; Mahapatra et al. 2006).

Both the familial and idiopathic, that is, not familial and of unknown cause, forms of PAH are associated with germ line mutations in the gene encoding the bone morphogenetic protein type 2 receptor (BMPR-2), *Bmpr2* (Thomson et al. 2001), which is part of the TGF-β superfamily. The TGF-β superfamily consists of cytokines and their receptors that contribute to the control of cell and tissue growth, inflammation, and neoplastic transformations (Newman et al. 2008). The BMPs were so named because they were first discovered

R. R. Vanderpool · N. C. Chesler (✉)
Department of Biomedical Engineering,
University of Wisconsin-Madison, 2146 Engineering Centers
Building, 1550 Engineering Drive, Madison, WI 53706, USA
e-mail: chesler@engr.wisc.edu

N. El-Bizri · M. Rabinovitch
Department of Pediatrics, Vera Moulton Wall Center
for Pulmonary Vascular Disease, Stanford University School
of Medicine, Stanford, CA 94305, USA

in repairing bone fractures (Urist 1965). At least three BMPs (BMP-4, -5, and -7) are present in the developing lung (Bellusci et al. 1996; King et al. 1994), and BMP-4 is an important regulator of epithelial proliferation and proximal-distal cell fate during lung morphogenesis (Cardoso 2001). BMPR-2 is activated by BMP-4, as well as BMPR-2 and BMP-7 (Newman et al. 2008).

In patients with familial and idiopathic PAH associated with BMPR-2 mutations, protein expression levels of BMPR-2 are decreased in pulmonary artery endothelial cells (Atkinson et al. 2002). Reduced BMPR-2 expression has also been documented in patients with secondary pulmonary hypertension due to chronic lung disease without a mutation and in experimental animal models of PAH (Takahashi et al. 2006). Thus, it has been suggested that BMPR-2 has an intracellular braking function that reduces pulmonary vascular cell proliferation (Atkinson et al. 2002) and that loss of normal BMPR-2 function leads to hyperplasia, especially in pulmonary arterioles (Newman et al. 2008).

The effects of BMPR-2 mutations are modulated in a dose-dependent way by BMPR-2 oligomerization with its co-receptor, most commonly BMPR-1A (Gilboa et al. 2000). BMPR-1A protein expression levels also are reduced in patients with familial and idiopathic PAH (Atkinson et al. 2002), and some patients with idiopathic or secondary PAH have reduced steady-state levels of BMPR-1A (Du et al. 2003). However, knockdown of *Bmrp1a* reduced proliferation in human pulmonary artery smooth muscle cells (SMCs) and resulted in resistance to apoptosis is vascular pericytes (El-Bizri et al. 2008). Indeed, in intact animals with reduced expression levels of BMPR-1A due to patchy *Bmpr1a* deletion, chronic hypoxia led to the same degree of pulmonary hypertension as wild-type littermates while markedly attenuating pulmonary arteriolar muscularization and reductions in arterial density of distal vessels, that is, pruning (El-Bizri et al. 2008). Thus, it is possible that reduced BMPR-1A expression levels found clinically in patients with PAH are protective for pulmonary vascular remodeling, especially in distal arterioles, and other modifier genes need to be upregulated to counter the protective effects of BMPR-1A loss of function.

An intriguing feature of these prior studies using intact mice with patchy deletion of *Bmpr1a* is that while pulmonary arteriolar muscularization and pruning are reduced in response to chronic hypoxia, the degree of pulmonary hypertension and right ventricular hypertrophy are unchanged from littermate controls (El-Bizri et al. 2008). This finding goes against the conventional wisdom that increased distal arterial muscularization and narrowing, and subsequent increases in pulmonary vascular resistance, are the primary determinant of right ventricular afterload and suggests that decreases in proximal arterial compliance, and subsequent increases in impedance, may play an important role in PAH progression.

Thus, we sought to investigate the impact of patchy deletion of *Bmpr1a* on pulmonary vascular impedance. We hypothesized that decreased arterial compliance from ectopic deposition of collagen (documented in (El-Bizri et al. 2008)) might account for increased right ventricular afterload in the absence of distal arteriolar remodeling. To test this hypothesis, pulsatile pressure-flow relationships were measured in isolated, ventilated, perfused lungs of *SM22α;TRE-Cre;R26R;Bmpr1a$^{flox/flox}$* (KO) mice and wild-type (WT) littermates following 21 days (hypoxia) and 0 days (control) of chronic hypoxia. We have previously reported on the utility of the isolated, ventilated, perfused lung system for measuring pulsatile pressure-flow relationships (Vanderpool et al. 2010). More recently, we demonstrated that by measuring pulsatile pressure-flow relationships at two different levels of resistance, we could predict not only the compliance but also the size and stiffness changes in the arteries that confer compliance, which we functionally have defined as "proximal" (Vanderpool et al. 2011). Two different levels of pulmonary vascular resistance can be achieved by acute administration of the rho kinase inhibitor Y27643, which lowers mean pulmonary artery pressure (mPAP) in isolated lungs (by dilating functionally distal arteries) (Vanderpool et al. 2011) as well as intact animals (Hyvelin et al. 2005; Nagaoka et al. 2004) but does not affect extralobar pulmonary artery SMC tone (Tabima and Chesler 2010b). Our results suggest that patchy deletion of *Bmpr1a* decreases dilatation and increases stiffening of functionally proximal arteries in response to hypoxia, which increases right ventricular afterload in the absence of distal, arteriolar muscularization, and narrowing.

2 Methods

2.1 Animal handling

Male and female *SM22α;TRE-Cre;R26R;Bmpr1a$^{flox/flox}$* (KO) mice and their wild-type (WT) littermates (El-Bizri et al. 2008) were used. Upon arrival, they were 30–40 weeks of age and 31.6 ± 5.3 g body weight. At the University of Wisconsin-Madison Biotron facility, mice were exposed to hypobaric hypoxia such that the partial pressure of O_2 was reduced by half, as previously described (Tuchscherer et al. 2007). While normobaric hypoxia is a more realistic model of chronic lung diseases, such as COPD, that can cause PAH, pathophysiological changes caused by normobaric hypoxia and hypobaric hypoxia in rodents are similar (Sheedy et al. 1996). Control mice (WT: $n = 5$; KO: $n = 6$) were exposed to 0 days of hypoxia, whereas hypoxic mice (WT: $n = 4$; KO: $n = 6$) were exposed to 21 days. This duration of hypoxia was chosen to match prior work with this strain (El-Bizri et al. 2008). The hypobaric chamber was opened for less than 30 min each week for cage changes and replenishing

food and water. At the end of the exposure, mice were euthanized with an intraperitoneal injection of 150 mg/kg body wt pentobarbital solution, which has been shown not to affect pulmonary hemodynamics (Benumof 1985; Mathers et al. 1977). All protocols and procedures were approved by the University of Wisconsin Institutional Animal Care and Use Committee.

2.2 Pulsatile pressure-flow studies

The isolated, ventilated, perfused mouse lung preparation was used for steady and pulsatile pressure-flow studies as previously developed and validated (Tuchscherer et al. 2006, 2007). In brief, following euthanasia, the trachea, pulmonary artery, and left atrium were cannulated for ventilation, perfusate inflow, and perfusate outflow, respectively. The tracheal cannula was inserted approximately halfway into the trachea. The PA cannula was positioned in main pulmonary artery with the tip just proximal to the first bifurcation. The left atrial catheter was inserted through the mitral valve and then withdrawn until the flares of the tip base obstructed the valve annulus. The lungs were ventilated with room air and perfused with heated RPMI 1640 cell culture medium with 3.5% Ficoll (an oncotic agent). A syringe pump (Cole-Parmer, Vernon Hills, IL) was used to create steady pulmonary vascular flow of perfusate, and a high-frequency oscillatory pump (Bose-Electro Force, Eden Prairie, MN) was used in parallel with the syringe pump to superimpose a pulsatile component on the pulmonary vascular flow. Pressure transducers (P75, Harvard Apparatus, Holliston, MA) measured the instantaneous pulmonary artery pressure (PAP) and left atrial pressure (LAP). Instantaneous flow rate (Q) was measured with an in-line flow meter (Transonic Systems, Inc., Ithaca, NY). Pressures and flows were monitored by continuous display on a computer and recorded at 200 Hz. Throughout the experiments, the system is visually checked for air bubbles and leaks that could affect the preparation and measurements. None were detected.

The pulsatile flow rate measurements were taken according to established methods after initial steady pressure-flow measurements of PAP, LAP and Q at 1 ml/min (Tuchscherer et al. 2006, 2007). In particular, pulsatile pressure-flow data were recorded for flow rates of the form $Q = 3 + 2 \sin (2\pi ft)$ ml/min at frequencies $f = 1, 2, 5, 10, 15,$ and 20 Hz. Flow oscillations of this magnitude (1–5 ml/min) could not be consistently generated with our system at frequencies above 20 Hz [~2.5 times the heart rate for mice, ~8 Hz in conscious unrestrained mice, (Schwenke et al. 2006)]. Following the collection of pulsatile pressure-flow data, steady pressure-flow measurements were taken at $Q = 1, 2, 3, 4,$ and 5 ml/min. All data were recorded with the lungs inflated at the end inspiratory pressure of 10 cm H_2O. Between protocols, the lungs were allowed to rest for 1 min with normal

ventilation (2–10 cm H_2O at 90 breaths/min) and a steady flow rate of $Q = 0.5$ ml/min.

Following measurements in a baseline SMC tone state, Y27632 (Sigma Chemical Company, St. Louis, MO), a rho kinase inhibitor, was added to the perfusate to a final concentration of 10^{-5} M to allow impedance measurements to be taken at two different levels of pulmonary vascular resistance (Vanderpool et al. 2011). Pulsatile pressure-flow measurements were taken 15 min after administration, followed by steady flow rate measurements. This time point was chosen to allow the effect of Y27632 to stabilize per prior reports (Nagaoka et al. 2004, 2005).

2.3 Calculations for pulsatile pressure-flow studies

Pulmonary vascular impedance magnitude (Z) and phase (θ) were calculated from one full sinusoidal cycle of $\Delta P = PAP–LAP$ and Q at each frequency tested ($f = 1, 2, 5, 10, 15,$ and 20 Hz). Input impedance Z_0 was calculated by averaging the impedance at the 0th harmonic ($f = 0$ Hz) from all tested frequencies. Characteristic impedance Z_C was calculated as the average of Z values between the first minimum (5 Hz) and the highest frequency imposed (20 Hz), and index of wave reflection R_W was calculated as $(Z_0 - Z_C)/(Z_0 + Z_C)$ (Nichols et al. 2005).

2.4 Estimation of proximal artery mechanics from a theoretical Z_C-mPAP relationship fit to experimental data

To estimate proximal artery size and stiffness, we fit the experimentally obtained dependence of Z_C on mean PAP to a theoretical relationship (Vanderpool et al. 2011). This theoretical relationship is based on the assumption that the proximal vasculature is a single, linearly elastic, homogeneous, thin-walled cylindrical artery with no wave reflections. With these assumptions, Z_C depends only on the artery wall elastic modulus (E), radius, and thickness, where radius and initial wall thickness depend on the mean transmural pressure, initial radius, and initial wall thickness (at zero pressure; or D_0 and h_0, respectively). With increasing pressure, the artery distends such that radius increases and wall thickness decreases by conservation of mass for a fixed artery length. For a particular set of E, D_0, and h_0 values, the relationship between mean PAP and Z_C can be found exactly (Vanderpool et al. 2011).

For each mouse, we derived the Z_C-mean PAP relationship from the baseline and Y27632 states. To do so assumes that proximal artery E, D_0, and h_0 do not change when hypoxic pulmonary vasoconstriction in arterioles is eliminated with Y27632, which is based on prior studies in which Y27632 had no significant effect on elastic modulus, diameter, or wall thickness of left pulmonary arteries (PAs) isolated

from C57BL6 mice (Tabima and Chesler 2010a). We then found the squared sum of error (SSE) for each combination of E, h_0, and D_0 in a defined space. Due to multiple local minimums and noise in the solution space, potential solutions were defined as those with an SSE of less than 10x the minimum SSE for each mouse. Mice with over 100 potential solutions with these constraints were excluded from further analysis. The SSE of the mice considered ranged from 1.0×10^{-8} to 1.6×10^{-5}. We further imposed the constraint that the ratio of stiffness (E in kPa) to wall thickness (h_0 in µm) would be greater than 1. Averages and standard deviations for the control KO, control WT, hypoxic KO, and hypoxic WT groups are presented.

As a secondary investigation of the solution space, k-means clustering was performed on all the potential solutions to provide an unsupervised classification of the solutions into groups (Jain et al. 1999; Jain 2010). The potential solutions were partitioned into 6 clusters. We report the centers of these clusters as well as the standard deviation of the clusters. These data provide some insight into differences in E, D_0, and h_0 between groups. Finally, we also applied this novel mouse-specific analysis technique to our previous Z_C-mean PAP data from control and hypoxic (10-day exposure) C57BL6 mouse lungs for which we previously used a group-wise analysis technique (Vanderpool et al. 2011).

3 Statistics

Absolute changes in study endpoints (mPAP, Z_0, Z_C and R_W) with regard to state (baseline vs. Y27632), hypoxic exposure (control vs. hypoxia), and strain (WT vs. KO) were analyzed using a generalized least squares (gls) for repeated measures with a compound symmetry structure. For Z_0, the main effects of hypoxic exposure and state and the interaction between those two factors were significant. However, the effects (main and interactive) of strain were not significant. This led to the construction of contrast matrices to investigate the changes in Z_0 as a function of exposure and state but not strain. For Z_C, again the main effects of hypoxic exposure and state were significant; however, this time there was a significant two-way interaction of hypoxic exposure and strain. From these significant interactions of factors, we constructed contrast matrices to investigate specific P values.

From the model-fitting analysis to estimate functionally proximal arterial size and stiffness, absolute changes in study endpoints (E, D_0, and h_0) with regard to hypoxic exposure (control vs. hypoxia) and strain (WT vs. KO) were analyzed using a generalized least squares (gls) for repeated measures with a compound symmetry structure. For D_0, the main effect of hypoxic exposure was significant that led to the construction of a contrast matrix to investigate the changes in D_0 as a function of exposure.

No violations of the normality assumption were found, and P values less than 0.05 were considered significant. All P values were two-sided, and all statistical analyses were performed using R software (R-project.org, version 2.5.1). All data are presented in terms of means ± standard deviation.

4 Results

Patchy deletion of *Bmpr1a* had no effect on mean pulmonary artery pressure (mPAP) at a steady flow rate of 3 ml/min in control or hypoxic lungs (Fig. 1). That is, mPAP was comparable in control WT and control KO lungs and greater but still similar in hypoxic WT and hypoxic KO lungs. In both strains, PAP decreased with Y27632 as expected (Fig. 1). As previously reported in C57BL6 mouse lungs exposed to 10 days of hypoxia (Vanderpool et al. 2011), mPAP decreased more in hypoxic lungs than in control lungs with Y27632 but not to control levels.

To determine the contribution of reduced expression of *Bmpr1a* to RV afterload, pulsatile pressure-flow relationships in both strains for control and hypoxic lungs with and without Y27632 were analyzed. All impedance spectra had the expected "L"-shape with a high amplitude at zero frequency and a rapid decline to low amplitudes at higher frequencies with moderate oscillations; the phase angles were negative at low frequencies and approached zero at higher frequencies (Fig. 2). In control lungs of both strains (Fig. 2, panels A and D), Z_0 decreased with Y27632, and the ratio of pressure to flow moduli shifted
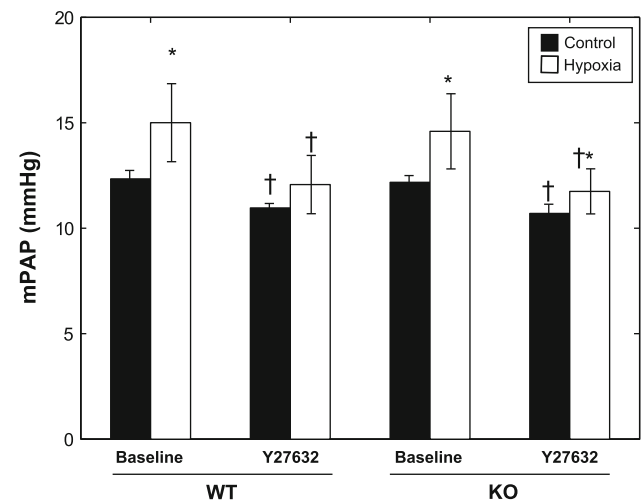
Fig. 1 Mean pulmonary artery pressure (mPAP) measured in response to steady flow ($Q = 3$ ml/min) in control and hypoxic KO (control: $n = 6$, hypoxic: $n = 5$) and WT (control: $n = 5$, hypoxic: $n = 4$) mouse lungs in the baseline SMC tone state and with Y27632. *$P < 0.05$ versus control; † $P < 0.05$ Y27632 versus *baseline*
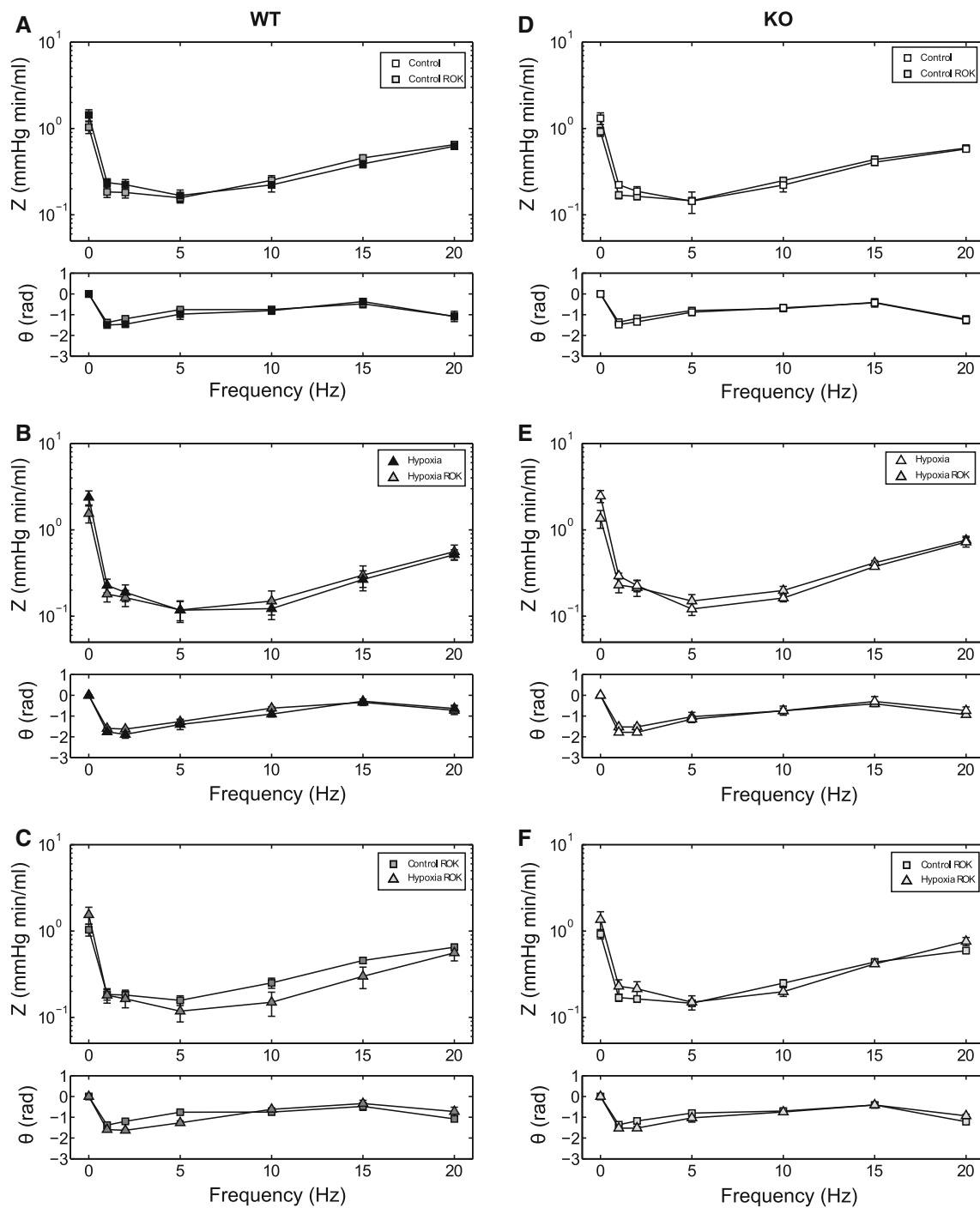
Fig. 2 Pulmonary vascular impedance magnitude (Z) and phase (θ) spectra in control and hypoxic KO and WT mouse lungs in the *baseline* smooth muscle tone state and with Y27632 from A) and D) control and B) and E) hypoxic mouse lungs (WT: A, B C; KO: D, E, F) in a *baseline* state and with Y27632

to higher pressures at high frequencies. As a consequence, Z_C tended to increase (Fig. 3). Phase angle was unaffected. In hypoxic lungs (Fig. 2, panel B), Z_0 decreased with Y27632 and the ratio of pressure to flow moduli at high frequencies did not change, resulting in no change of Z_C (Fig. 3).

The increase in Z_0 and decrease in impedance magnitude at higher frequencies with chronic hypoxia, either with or without Y27632, resulted in a crossover between the two spectra. Hypoxia tended to affect phase angle, but no significant effect as a function of frequency was found (Fig. 2, panels C and F with Y27632 shown only).

Fig. 3 Input impedance (Z_0; *top*) and characteristic impedance (Z_C; *bottom*) for each individual control and hypoxic mouse in both the WT and KO strains in the *baseline* SMC tone state and with Y27632. *$P < 0.05$ versus 0-day; †$P < 0.05$ Y27632 versus *baseline*
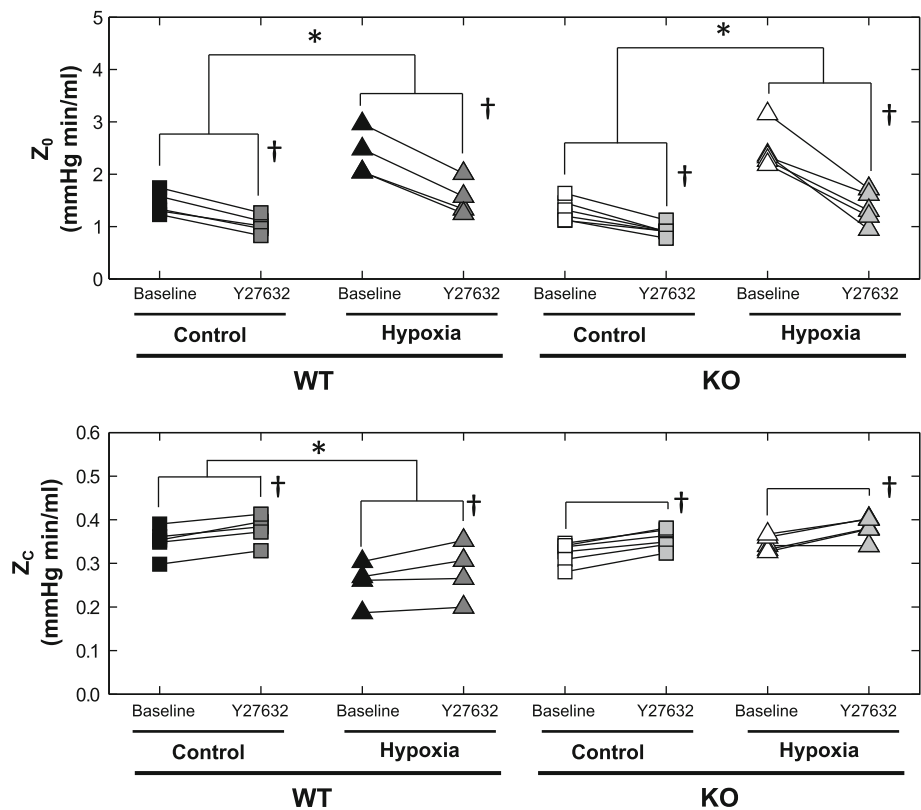
The effects of the patchy deletion of *Bmpr1a* on Z_0 and Z_C are more easily understood by direct comparison. As shown in Fig. 3 (top panel), patchy deletion of *Bmpr1a* did not affect the increase in input impedance Z_0 with chronic hypoxia or the decrease in Z_0 with Y27632. However, patchy deletion of *Bmpr1a* eliminated the decrease in characteristic impedance Z_C with chronic hypoxia (bottom panel).

The contribution of functionally proximal arterial size and stiffness to pulsatile pressure-flow measurements in the isolated lungs was investigated using the theoretical relationships between Z_C and mPAP. Theoretical Z_C values were calculated for elastic modulus, E, from 20 to 250 kPa, wall thickness, h_0, from 20 to 250 µm and inner diameter, D_0, from 500 to 2,000 µm for each mouse. Representative solutions for each strain and exposure were plotted atop the experimental data (Fig. 4). In the control mice for all the strains, the theoretical Z_C fit the experimental data well (Fig. 4, first row). Following chronic hypoxia, the fitting was more variable and strain dependent (Fig. 4, second row). In the *SM22α;TRE-Cre;R26R;Bmpr1a$^{flox/flox}$* WT and KO mice exposed to 21 days of chronic hypoxia, experimental data were well fit by the theoretical Z_C. In the C57BL6 mice exposed to 10 days of chronic hypoxia, Y27632 had a larger impact on Z_C, causing poor fit with the theoretical Z_C.

The theoretical calculation of D_0, h_0, and E as well as the clustering results (similar to theoretical solutions; not

shown) suggests that in all strains of mice, hypoxia increases D_0, h_0, and E (Table 1). These results also suggest that patchy deletion of Bmpr1a leads to somewhat smaller arteries with lower elastic moduli under control conditions. With exposure to chronic hypoxia, the deletion limits the increases in diameter and wall thickness that occur with chronic hypoxia but potentiates the increase in elastic modulus (Table 1).

5 Discussion

The main findings of the present study are that *Bmpr1a* deficiency does not limit the increase in pulmonary vascular resistance in response to chronic hypoxia, despite less marked arteriolar muscularization and pruning, and that *Bmpr1a* deficiency potentiates functionally proximal arterial remodeling, via decreased dilatation and increased stiffening, to increase RV afterload.

Previously, histological studies demonstrated that chronic hypoxia-induced increases in muscularization and reductions in arterial density of distal vessels (<200 µm) are attenuated by patchy deletion of BMPR1a in SMC (El-Bizri et al. 2008). It is unclear why we did not detect functional changes in steady flow hemodynamics (i.e., mPAP and pulmonary vascular resistance) despite reduced arteriolar remodeling

Fig. 4 Representative experimental and theoretical Z_C-mean PAP relationships for each strain (C57BL6, WT and KO) and hypoxic exposure (C57BL6: 10 days, WT and KO: 21 days) when a theoretical D_0, h_0 and E is found for each individual mouse. The extrema of the solution spaces for the theoretical Z_C-mPAP relationships are shown by the bounding areas
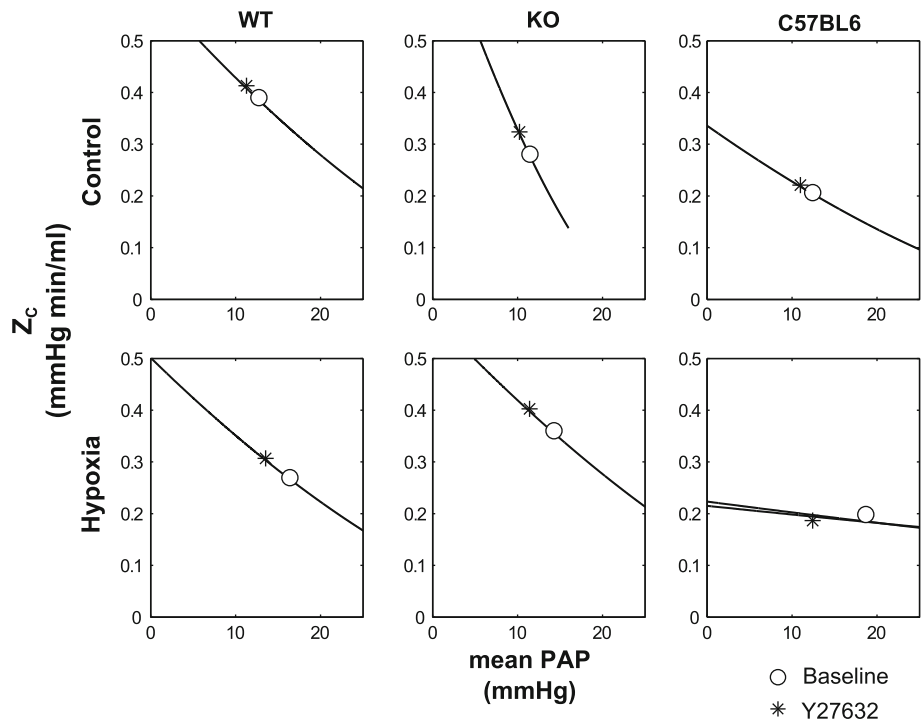
Table 1 Average theoretical D_0, h_0, and E for each strain (WT and KO BMPR1a and C57BL6) and exposure (control and hypoxia)

Only mice for which the number of solutions was less than 100 are included here

		Exposure length	Theoretical solutions		
			D_0	h_0	E
WT BMPR1a	Control ($n = 4$)		750 ± 86	39 ± 2	115 ± 43
	Hypoxia ($n = 3$)	21 days	1001 ± 325	61 ± 32	134 ± 31
KO BMPR1a	Control ($n = 6$)		683 ± 142	38 ± 14	80 ± 24
	Hypoxia ($n = 4$)	21 days	861 ± 113	50 ± 11	145 ± 34
C57BL6	Control ($n = 4$)		1108 ± 284	59 ± 11	147 ± 42
	Hypoxia ($n = 1$)	10 days	1875	187	237

in the KO strain. Arteriolar remodeling was measured from histological sections of lungs in which persistent hypoxic pulmonary vasoconstriction was not eliminated prior to fixation (El-Bizri et al. 2008). However, acute administration of Y27632, which does eliminate persistent hypoxic pulmonary vasoconstriction (Nagaoka et al. 2004), also did not lead to a functional difference in resistance between the strains. Possibly, the degree of reduction in arteriolar remodeling in the KO mice may be too subtle to have functional effect at the lower flow rates used ex vivo. An important difference between in vivo and ex vivo conditions is the ~3-fold lower than physiological flow rate ex vivo (Tabima et al. 2010). At more physiological mean flow rates, lungs from KO mice may have had lower mPAP and resistance than those from WT mice. However, at high mean flow rates, the isolated lungs became edematous in our hands so we could not test this explanation for the discrepancy between the histological and functional findings regarding the effects of hypoxia on the distal vasculature.

Loss of arterial compliance, or arterial stiffening, is thought to be key to PAH progression through two mechanisms: increased arteriolar cyclic strain damage and increased pulmonary vascular impedance. The former causes SMC proliferation and arterial narrowing (Li et al. 2009), whereas the latter increases RV afterload (Milnor et al. 1969). Indeed, large pulmonary artery stiffening accounts for over a third of the RV workload increase with pulmonary hypertension (Stenmark et al. 2006). Here, we sought to determine whether proximal artery stiffening in the absence of arteriolar histological changes might explain increased RV systolic pressures.

The consequences of pulmonary arterial stiffening for RV afterload can be quantified in isolated, ventilated perfused lungs by analyzing the Z_C-mPAP relationship. In this ex vivo preparation, chronic hypoxia decreases Z_C because pressure-related increases in functionally proximal arterial diameters decrease Z_C more than stiffening increases Z_C (Vanderpool et al. 2011, 2010). By fitting the Z_C-mPAP data to a

theoretical curve, the relative changes in diameter and elastic modulus, as well as wall thickness, can be predicted. This approach was previously validated using microcomputed tomography imaging of the right main extralobar artery (Vanderpool et al. 2011). Here, we used novel mouse-specific approach and obtained results similar to our prior findings using a group-average approach (Vanderpool et al. 2011). Our findings of increased stiffness and wall thickness are consistent with isolated extralobar pulmonary artery mechanical tests (Tabima and Chesler 2010a). However, goodness-of-fit was exposure condition and strain specific, with poor fits for the C57BL6 mice following 10 days of chronic hypoxia. A contributing factor to the goodness-of-fit may be the different lengths of exposure to chronic hypoxia between the strains.

Using the mouse-specific approach in the KO and WT mice, we found here that in mice with reduced *Bmpr1a* expression, 21 days of chronic hypoxic exposure had no effect on Z_C. Our theoretical analysis suggests that the mechanism is a smaller increase in diameter coupled with a larger increase in elastic modulus. These two findings can both be explained by adventitial or periadventitial collagen accumulation. El-Bizri et al. found increased periadventitial deposition of collagen in small- to mid-sized arteries ($\sim$400 μm diameter) in association with fragmented ectopic deposition of elastin in the KO strain in response to hypoxia (El-Bizri et al. 2008). Also, we have previously shown that vascular collagen is critical to hypoxia-induced pulmonary arterial stiffening (Ooi et al. 2010).

It is interesting to note that since we did not obtain impedance measurements above 20 Hz, which is only twice the native heart rate of the mouse (Schwenke et al.), Z_C reflects the impedance of the intermediate arteries not the largest, most proximal, extralobar arteries. Information about the largest, most proximal, extralobar arteries only can be obtained at frequencies 4–10 times higher than the native heart rate (Milnor 1989). Thus, our results coupled with the prior El-Bizri results suggest that localized, compensatory remodeling in the intermediate proximal arteries (200–600 μm in diameter) may be critical to increasing RV afterload with patchy deletion of BMPR1a.

6 Limitations

As noted above, these results from isolated, ventilated and perfused lungs cannot be directly compared to in vivo measurements due to the low mean flow rate; in addition, the perfusate viscosity is lower than physiological (by 3- to 4-fold) and flow rate waveform does not mimic the natural waveform. Since Z_C is pressure dependent (Vanderpool et al. 2011), the differences in flow rate and viscosity affect the magnitude of Z_C. In addition, our calculations of impedance spectra are based on pulsatile waveforms with single frequencies that were imposed in a fixed order. Therefore, time-dependent effects could have affected our higher frequency data more than our lower frequency data. However, given the short duration of all pulsatile flow trials (66 s in total for three sequential trials from $f = 1$ to 20 Hz), this effect is likely to be small.

An additional limitation is that the number of animals in each group is relatively small. In our prior work with the isolated, ventilated and perfused lung system, we typically use sample sizes of five (Vanderpool et al. 2011) or six (Tuchscherer et al. 2006, 2007; Vanderpool et al. 2010). Here, we were able to detect statistically significant differences with even fewer animals, which speaks to the consistency of our approach. The criteria we used to define an acceptable model fit severely limited number of C57BL6 mice exposed to hypoxia that we could analyze theoretically; however, this limitation did not affect the $SM22\alpha;TRE\text{-}Cre;R26R;Bmpr1a^{flox/flox}$ KO and WT mice.

Finally, an important limitation is that we were unable to isolate and mechanically test individual intermediate-sized arteries (200–600 μm in diameter) that our results suggest dilate less and stiffen more in response to hypoxia in the KO mice. Similarly, we were unable to harvest these arteries and biochemically measure collagen and elastin content as we have done previously with the extralobar PAs ($\sim$800–1,000 μm in diameter) (Ooi et al. 2010). By combining our current functional measurements with detailed structural and morphometric data in the future, we hope to define the size and location of arteries that confer compliance and resistance to the pulmonary vasculature in both healthy and diseased states.

7 Conclusion

We conclude that reduced *Bmpr1a* expression does not affect the response of the arteries that control resistance to hypoxia, such that pulmonary vascular resistance increases in response to chronic hypoxia as much in mice with BMPR-1A loss of function as in mice with normal BMPR-1A function. The mechanisms by which this increase in resistance occurs in the absence of significant arteriolar muscularization and pruning remain to be elucidated. We also conclude that reduced *Bmpr1a* expression potentiates the response of the arteries that control compliance to hypoxia such that they dilate less and become more stiff, thus increasing RV afterload. Therefore, these results suggest reduced BMPR-1A expression levels found clinically are only protective for some aspects of pulmonary vascular remodeling and that their effects of proximal arteries may in fact promote the progression of PAH without the need to invoke modifier genes that counteract BMPR-1A loss of function.

References

Atkinson C, Stewart S, Upton PD, Machado R, Thomson JR, Trembath RC, Morrell NW (2002) Primary pulmonary hypertension is associated with reduced pulmonary vascular expression of type II bone morphogenetic protein receptor. Circulation 105(14):1672–1678

Bellusci S, Henderson R, Winnier G, Oikawa T, Hogan BL (1996) Evidence from normal expression and targeted misexpression that bone morphogenetic protein (Bmp-4) plays a role in mouse embryonic lung morphogenesis. Development 122(6):1693–1702

Benumof J (1985) One-lung ventilation and hypoxic pulmonary vasoconstriction: implications for anesthetic management. Anesth Analg 64(8):821–833

Cardoso WV (2001) Molecular regulation of lung development. Annu Rev Physiol 63:471–494. doi:10.1146/annurev.physiol.63.1.47163/1/471[pii]

Du L, Sullivan CC, Chu D, Cho AJ, Kido M, Wolf PL, Yuan JX, Deutsch R, Jamieson SW, Thistlethwaite PA (2003) Signaling molecules in nonfamilial pulmonary hypertension. N Engl J Med 348(6):500–509. doi:348/6/500[pii]10.1056/NEJMoa021650

El-Bizri N, Wang L, Merklinger S, Guignabert C, Desai T, Urashima T, Sheikh A, Knutsen R, Mecham R, Mishina Y, Rabinovitch M (2008) Smooth muscle protein 22alpha-mediated patchy deletion of Bmpr1a impairs cardiac contractility but protects against pulmonary vascular remodeling. Circ Res 102(3):380–388. doi:CIRCRESAHA.107.161059[pii]10.1161/CIRCRESAHA.107.161059

Gan CT, Lankhaar JW, Westerhof N, Marcus JT, Becker A, Twisk JW, Boonstra A, Postmus PE, Vonk-Noordegraaf A (2007) Noninvasively assessed pulmonary artery stiffness predicts mortality in pulmonary arterial hypertension. Chest 132(6):1906–1912

Gilboa L, Nohe A, Geissendorfer T, Sebald W, Henis YI, Knaus P (2000) Bone morphogenetic protein receptor complexes on the surface of live cells: a new oligomerization mode for serine/threonine kinase receptors. Mol Biol Cell 11(3):1023–1035

Hyvelin JM, Howell K, Nichol A, Costello CM, Preston RJ, McLoughlin P (2005) Inhibition of Rho-kinase attenuates hypoxia-induced angiogenesis in the pulmonary circulation. Circ Res 97(2):185–191

Jain AK (2010) Data clustering: 50 years beyond K-means. Pattern Recognit Lett 31:651–666

Jain AK, Murty MN, Flynn PJ (1999) Data clustering: a review. ACM Comput Surv 31(3):264–323

King JA, Marker PC, Seung KJ, Kingsley DM (1994) BMP5 and the molecular, skeletal, and soft-tissue alterations in short ear mice. Dev Biol 166(1):112–122. doi:S0012-1606(84)71300-5[pii]10.1006/dbio.1994.1300

Li F, Xia W, Yuan S, Sun R (2009) Acute inhibition of Rho-kinase attenuates pulmonary hypertension in patients with congenital heart disease. Pediatr Cardiol 30(3):363–366

Mahapatra S, Nishimura R, Sorajja P, Cha S, McGoon M (2006) Relationship of pulmonary arterial capacitance and mortality in idiopathic pulmonary arterial hypertension. J Am Coll Cardiol 47(4):799–803

Mathers J, Benumof J, Wahrenbrock E (1977) General anesthetics and regional hypoxic pulmonary vasoconstriction. Anesthesiology 46(2):111–114

McLaughlin VV, Archer SL, Badesch DB, Barst RJ, Farber HW, Lindner JR, Mathier MA, McGoon MD, Park MH, Rosenson RS, Rubin

LJ, Tapson VF, Varga J (2009) ACCF/AHA 2009 expert consensus document on pulmonary hypertension a report of the American College of Cardiology Foundation Task Force on Expert Consensus Documents and the American Heart Association developed in collaboration with the American College of Chest Physicians; American Thoracic Society, Inc.; and the Pulmonary Hypertension Association. J Am Coll Cardiol 53(17):1573–1619. doi:S0735-1097(09)00142-9[pii]10.1016/j.jacc.2009.01.004

Milnor WR (1989) Hemodynamics, 2nd edn. Williams & Wilkins, Baltimore

Milnor WR, Conti CR, Lewis KB, O'Rourke MF (1969) Pulmonary arterial pulse wave velocity and impedance in man. Circ Res 25(6):637–649

Nagaoka T, Fagan KA, Gebb SA, Morris KG, Suzuki T, Shimokawa H, McMurtry IF, Oka M (2005) Inhaled Rho kinase inhibitors are potent and selective vasodilators in rat pulmonary hypertension. Am J Respir Crit care Med 171(5):494–499

Nagaoka T, Morio Y, Casanova N, Bauer N, Gebb S, McMurtry I, Oka M (2004) Rho/Rho kinase signaling mediates increased basal pulmonary vascular tone in chronically hypoxic rats. Am J Physiol Lung Cell Mol Physiol 287(4):L665–672

Newman JH, Phillips JA 3rd, Loyd JE (2008) Narrative review: the enigma of pulmonary arterial hypertension: new insights from genetic studies. Ann Intern Med 148(4):278–283. doi:148/4/278[pii]

Nichols WW, O'Rourke MF, Hartley C, McDonald DA (2005) McDonald's blood flow in arteries : theoretical, experimental, and clinical principles, 5th edn. Arnold, London

Ooi CY, Wang Z, Tabima DM, Eickhoff JC, Chesler NC (2010) The role of collagen in extralobar pulmonary artery stiffening in response to hypoxia-induced pulmonary hypertension. Am J Physiol Heart Circ Physiol 299(6): H1823–1831. doi:ajpheart.00493.2009[pii]10.1152/ajpheart.00493.2009

Schwenke DO, Pearson JT, Mori H, Shirai M (2006) Long-term monitoring of pulmonary arterial pressure in conscious, unrestrained mice. J Pharmacol Toxicol Methods 53(3):277–283. doi:S1056-8719(05)00142-5[pii]10.1016/j.vascn.2005.11.003

Sheedy W, Thompson JS, Morice AH (1996) A comparison of pathophysiological changes during hypobaric and normobaric hypoxia in rats. Respiration 63(4):217–222

Stenmark KR, Fagan KA, Frid MG (2006) Hypoxia-induced pulmonary vascular remodeling - cellular and molecular mechanisms. Circ Res 99(7):675–691. doi:10.1161/01.RES.0000243584.45145.3f

Tabima D, Chesler N (2010) The effects of vasoactivity and hypoxic pulmonary hypertension on extralobar pulmonary artery biomechanics. J Biomech 43(10):1864–1869. doi:S0021-9290(10)00178-8[pii]10.1016/j.jbiomech.2010.03.033

Tabima DM, Chesler NC (2010) The effects of vasoactivity and hypoxic pulmonary hypertension on extralobar pulmonary artery biomechanics. J Biomech 43(10):1864–1869. doi:S0021-9290(10)00178-8[pii]10.1016/j.jbiomech.2010.03.033

Tabima DM, Hacker TA, Chesler NC (2010) Measuring right ventricular function in the normal and hypertensive mouse hearts using admittance-derived pressure-volume loops. Am J Physiol Heart Circ Physiol. doi:ajpheart.00805.2010[pii]10.1152/ajpheart.00805.2010

Takahashi H, Goto N, Kojima Y, Tsuda Y, Morio Y, Muramatsu M, Fukuchi Y (2006) Downregulation of type II bone morphogenetic protein receptor in hypoxic pulmonary hypertension. Am J Physiol Lung Cell Mol Physiol 290(3): L450–458. doi:00206.2005[pii]10.1152/ajplung.00206.2005

Thomson J, Machado R, Pauciulo M, Morgan N, Yacoub M, Corris P, McNeil K, Loyd J, Nichols W, Trembath R (2001) Familial and sporadic primary pulmonary hypertension is caused by BMPR2 gene mutations resulting in haploinsufficiency of the bone

morphogenetic protein tùype II receptor. J Heart Lung Transplant 20(2):149. doi:S1053-2498(01)00259-5[pii]

Tuchscherer HA, Vanderpool RR, Chesler NC (2007) Pulmonary vascular remodeling in isolated mouse lungs: effects on pulsatile pressure-flow relationships. J Biomech 40(5):993–1001

Tuchscherer HA, Webster EB, Chesler NC (2006) Pulmonary vascular resistance and impedance in isolated mouse lungs: effects of pulmonary emboli. Ann Biomed Eng 34(4):660–668

Urist MR (1965) Bone: formation by autoinduction. Science 150(698): 893–899

Vanderpool RR, Kim AR, Molthen R, Chesler NC (2011) Effects of acute Rho kinase inhibition on chronic hypoxia-induced changes in proximal and distal pulmonary arterial structure and function. J Appl Physiol 110(1):188–198. doi:japplphysiol.00533.2010[pii]10.1152/japplphysiol.00533.2010

Vanderpool RR, Naeije R, Chesler NC (2010) Impedance in isolated mouse lungs for the determination of site of action of vasoactive agents and disease. Ann Biomed Eng 38(5):1854–1861. doi:10.1007/s10439-010-9960-2